



The 3-D reconstruction of medieval wetland reclamation through electromagnetic induction survey

Philippe De Smedt¹, Marc Van Meirvenne¹, Davy Herremans², Jeroen De Reu², Timothy Saey¹, Eef Meerschman¹, Philippe Crombé² & Wim De Clercq²

¹Department of Soil Management, Faculty of Bioscience Engineering, Ghent University, Coupure 653, 9000 Gent, Belgium,

²Department of Archaeology, Faculty of Arts and Philosophy, Ghent University, Sint-Pietersnieuwstraat 35 UFO, 9000 Gent, Belgium.

Received
27 December 2012

Accepted
5 March 2013

Published
21 March 2013

SUBJECT AREAS:
GEOLOGY
APPLIED PHYSICS
SOLID EARTH SCIENCES
ENVIRONMENTAL SCIENCES

Correspondence and requests for materials should be addressed to P.D.S. (Philippe.DeSmedt@UGent.be)

Studies of past human-landscape interactions rely upon the integration of archaeological, biological and geological information within their geographical context. However, detecting the often ephemeral traces of human activities at a landscape scale remains difficult with conventional archaeological field survey. Geophysical methods offer a solution by bridging the gap between point finds and the surrounding landscape, but these surveys often solely target archaeological features. Here we show how simultaneous mapping of multiple physical soil properties with a high resolution multi-receiver electromagnetic induction (EMI) survey permits a reconstruction of the three-dimensional layout and pedological setting of a medieval reclaimed landscape in Flanders (Belgium). Combined with limited and directed excavations, the results offer a unique insight into the way such marginal landscapes were reclaimed and occupied during the Middle Ages. This approach provides a robust foundation for unravelling complex historical landscapes and will enhance our understanding of past human-landscape interactions.

In landscape archaeology, geophysical methods are increasingly being applied to conduct large area surveys¹. Although these techniques allow obtaining high-resolution archaeological information at a landscape-scale²⁻⁴, they often neglect natural landscape variations. To fully understand the driving mechanisms behind human land-use, the integration of pedological and geomorphological information in these prospection stages is crucial.

In Europe, one of the most characteristic examples of past human-landscape interaction, is the reclamation of wetlands and forest that followed the urbanisation of the historical County of Flanders (Fig. 1b). During Medieval periods, these lowlands experienced a considerable population growth, making the County one of the most densely populated areas in Europe between the 11th and the 15th centuries⁵. To meet the demands of emerging cities, such as Ghent, Bruges and Ypres⁶, entire natural landscapes were reclaimed, transforming these into a landscape of dynamic exploitation⁷. The ruling Counts of Flanders spearheaded this evolution by endowing feudal lords with lands, while abbeyes were deliberately installed on marginal land all over Flanders.

More recent, natural processes (e.g. flooding) and modernisation have altered the cultural landscape of medieval Flanders, leaving the nature and exact layout of these designed landscapes largely unknown⁸. Although social formation and economic exploitation of reclaimed landscapes during the High Middle Ages is, to some extent, documented in historical and cartographical sources, archaeological evidence remains scarce. One of the main reasons for this scarcity is that traditional investigations have focused on recovering architectural remains rather than situating the structures within their broader environmental contexts. By focusing on elite residences and monastic buildings, archaeological investigations have contributed to the biased image of medieval settlement landscapes that still prevails.

The situation was no different for the Cistercian abbey of Boudelo located in the north of the County of Flanders (Fig. 1b). In 1197, a small religious community settled in this area⁹, which at that time was an outback of the County, dominated by marshes and wetlands. Early historical accounts, such as those by monks from the Abbey of Clairvaux in Bourgogne (France), give testament to the harsh environmental conditions. They describe life at Boudelo as *pauper* and *misserimus*: poor and full of misery¹⁰. However, the community improved its property by cultivating the surrounding land. Between the 13th and 16th centuries, the monastic estate expanded to over 1000 ha, making the community one of the leading cultivators in the County. After religious as well as

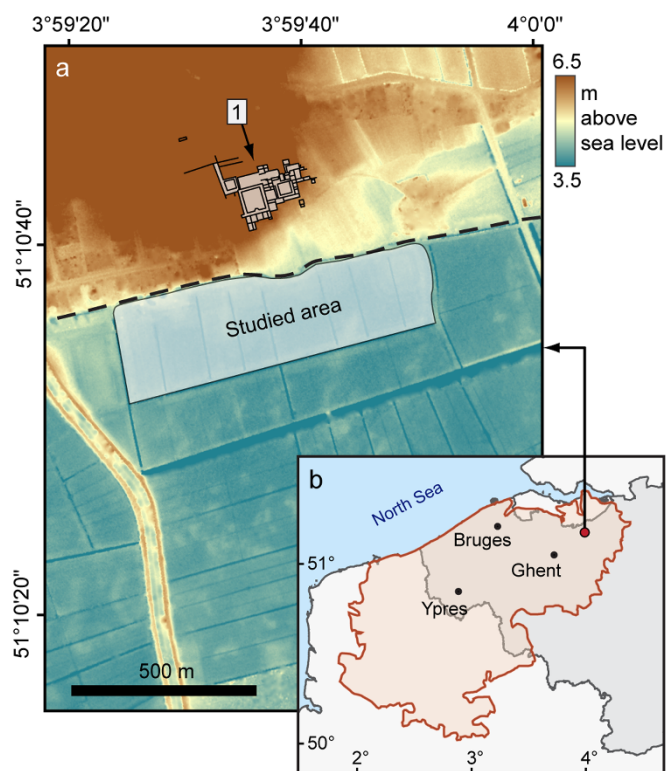


Figure 1 | Location and historical context of the site. (a), The location and elevation³² of the study area with indication of the excavated Abbey of Boudelo (1). The dashed line represents the boundary between the palaeolake (to its south) and the coversand ridge (to its north). (b), Location of the studied area (red dot) within the late medieval County of Flanders (orange boundary) and the current state boundary of Belgium. Maps composed in ESRI ArcMAP 9.3.1.

military struggles and successive floods, the monks were forced to abandon their grounds in Boudelo in 1578. They found refuge in Ghent and the monastic buildings were sold and dismantled.

Although the extensive reclamation strategy of the abbey is attested in historical records mentioning embankment, drainage, stockbreeding, extraction of peat and clay, and the production of building ceramics, it remains hidden in the archaeological record. Excavations in the 1970s revealed the remnants of the cloister range and the abbey church, leading archaeologists to interpret the abbey grounds as limited to the coversand ridge¹¹ (Fig. 1a). The border of the monastic precinct was believed to coincide with the edge of a Late Glacial palaeolake, which was, and remains, a waterlogged environment dominated by peat and lime-rich lacustrine deposits (Fig. 1, Supplementary Fig. 1–2). However, in 2011 an electromagnetic induction (EMI) survey of this wetland area drastically altered this interpretation, as it unveiled traces of the abbey's outer court that once was part of the monastic precinct; a previously unknown designed landscape from which the monks directed their cultivation of the surrounding area.

The multi-receiver EMI sensor we used, allows simultaneously recording the apparent electrical conductivity (σ_a) and apparent magnetic susceptibility (κ_a) of four different soil volumes¹². Whereas in non-saline environments σ_a can be directly related to soil texture (clay, silt, sand), and is influenced by soil organic matter and water content^{13,14}, κ_a anomalies are often the result from ferrimagnetic soil enrichment^{15,16}, the anthropogenic disturbance¹⁷ of top soils (e.g. ditches), or the heating of soil¹⁸ (e.g. hearths, bricks). This contrasts to other geophysical survey techniques, such as magnetometry¹⁹ and ground penetrating radar²⁰, that each target only one

specific variable and are inadequate to appreciate the full range of soil textural variability of surveyed sites. However, integrating electrical and magnetic soil properties in a single EMI survey allows targeting the pedological, geomorphological and archaeological variations jointly. By simultaneously mapping multiple soil volumes with a multi-receiver instrument, vertical discrimination potential is added to the electrical and magnetic data layers.

Results

The σ_a data revealed a complex environment with alternations of highly conductive lake deposits and peat accumulations (Fig. 2a). Apart from scarce sandy outcrops the measurements indicate a buried marshland influenced by long lasting, saturated conditions. Several ditches were revealed as highly conductive anomalies surrounding the entire survey area and enclosing two smaller zones. The high conductivity of the ditches is caused by high concentrations of fine-grained sediments (clay) and peat that contrast with the more resistive underlying sand. The extent and layout of the ditches and their persisting in the present-day drainage system indicates considerable medieval investment in reclaiming this wetland. The two smaller enclosed compounds appear to centre around sandy areas within the larger enclosure (S1 and S2 in Fig. 2). On the central platform within each compound, the κ_a measurements showed highly magnetic structures (Fig. 2b and d). At the easternmost site (S1), at least 18 features with a minimum diameter of 1 m, suggest the layout of a rectangular structure some 20 m by 30 m square (Fig. 2d). A central structure can be observed at the western site (S2) (Fig. 2b). Here, the elevated κ_a of the ditches indicates their infilling with brick and other magnetic debris, whereas a trail of high κ_a values leading north suggests displacing rubble towards the sand ridge.

To interpret and complement the geophysical data excavation trenches were laid out across the ditches and the central structure of each site (Supplementary Fig. 1–2). At both sites brick structures were found, as indicated by the κ_a measurements (Fig. 2b–e). These were identified as block foundations used to support a larger, most likely wooden, structure and to keep it away from the saturated soil. While a functional interpretation of S2 has been hampered by the poor conservation of the excavated building remains, the central structure at S1 has been interpreted as a large monastic barn. The morphology of the sandy outcrop, combined with elevated ground water levels caused instability of the foundations leading to the collapse of the building. The excavated material culture and construction materials indicate that both sites were occupied between the 13th and the early 14th centuries. This links their abandonment to a period of documented increased flooding in the region²¹.

Based on the σ_a and excavation data, we modelled the relative medieval topography of the site^{22,23}. Although the heterogeneity of the ditch infillings, the peat layers and the targeted sandy layers limited the precision of this modelling procedure, an accurate model of the medieval surface was obtained. At 84 validation locations in the excavation trench at S2 a RMSEE of 0.37 cm and a Spearman correlation coefficient of 0.80 was obtained between the observed (Fig. 3a) and modelled (Fig. 3b) depths to the archaeological layers. Although the selection of the validation observations was not statistically random, the results confirmed the relative model correspondence to the medieval topography. A comparison of the modelled data to the observed surface along the validation transect (Fig. 3), shows the smoothing effect on the modelled data, but confirms the accurate representation of the targeted archaeological layers.

By integrating the κ_a data into the model, a comprehensive reconstruction of the reclaimed landscape was obtained (Fig. 4). Both S1 and S2 are located on prominently higher and sandier locations, which are connected to the bordering sand ridge in the north. However, while the barn (at S1) was built on an existing sandy

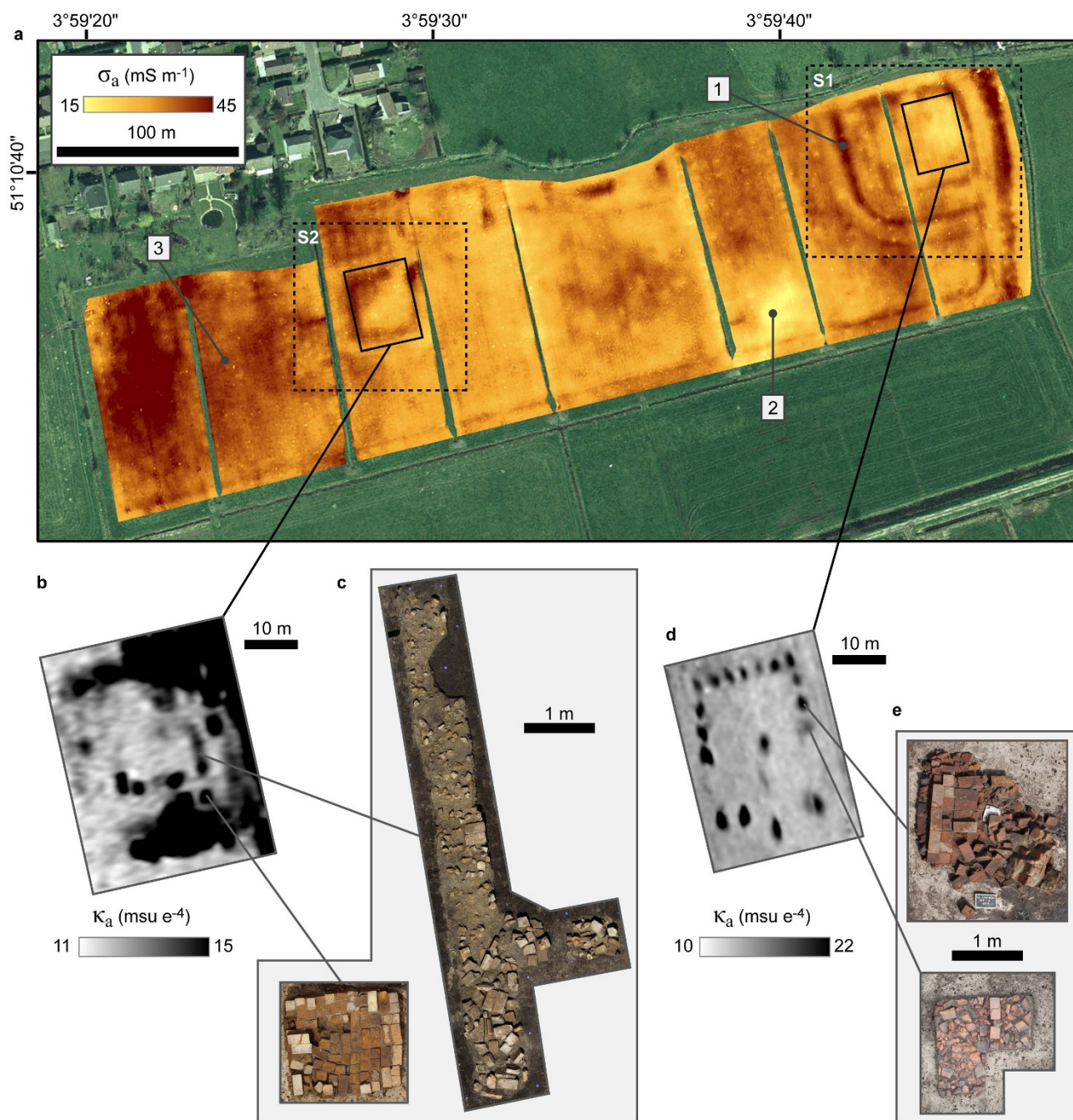


Figure 2 | Electromagnetic induction data and excavated structures. (a), 1 m HCP σ_a data of the study area, plotted on an orthophotograph of the study area³³, with indication of a man-made ditch (1), a sandy outcrop (2) and an area with accumulated peat and lacustrine deposits (3). The dashed lines indicate both moated sites S1 and S2. (b), 2 m HCP κ_a data of the platform of S2, showing the central building and the magnetic disturbances caused by rubble in the ditches and leading towards the north (Supplementary Fig. 2). (c, e), Orthophotos of the brick foundations as revealed by the excavations at S2 (c) and S1 (e). (d), 2 m HCP κ_a data showing traces of 18 brick block foundations on the platform in S1. Maps composed in ESRI ArcMAP 9.3.1.

outcrop, excavations showed that S2 was artificially raised (Supplementary Figure 2d) by removing sand from the ditches and the adjacent sand ridge. The design of both sites confirms a link to the nearby abbey buildings as their topographic position was chosen or altered in order to allow easy access to the sand ridge. The ditch enclosing the area was largest east of S1 with a width of up to 10 m and a depth of 1.5 m below the surface (Supplementary Figure 1d). Here, a larger drainage capacity was needed, as the ditch was part of the complex-wide drainage system. This large ditch also expressed a separation between the inside and outside worlds; a symbolic reminder of the separation between religious and secular life²⁴. The ditches circling S2

and the remainder of S1 rarely surpassed a depth of 1 m and had a width ranging from 2 m to 8 m (Supplementary Fig. 1d and 2e). These wide ditches did not only supply additional drainage for the enclosed zones, but also formed a physical boundary that embodied aspects of identity and status²⁵. Individual compounds, such as S1 and S2, with an (artificially) raised platform and enclosed by ditches, can be defined as late-medieval moated sites²⁵. In addition, the surface model shows dykes neighbouring the ditches that add to the embankment and visibility of both moated sites. Remnants of these earthworks were attested in the excavation trenches, either still *in situ* or thrown into the moat ditches (Supplementary Figure 2e).

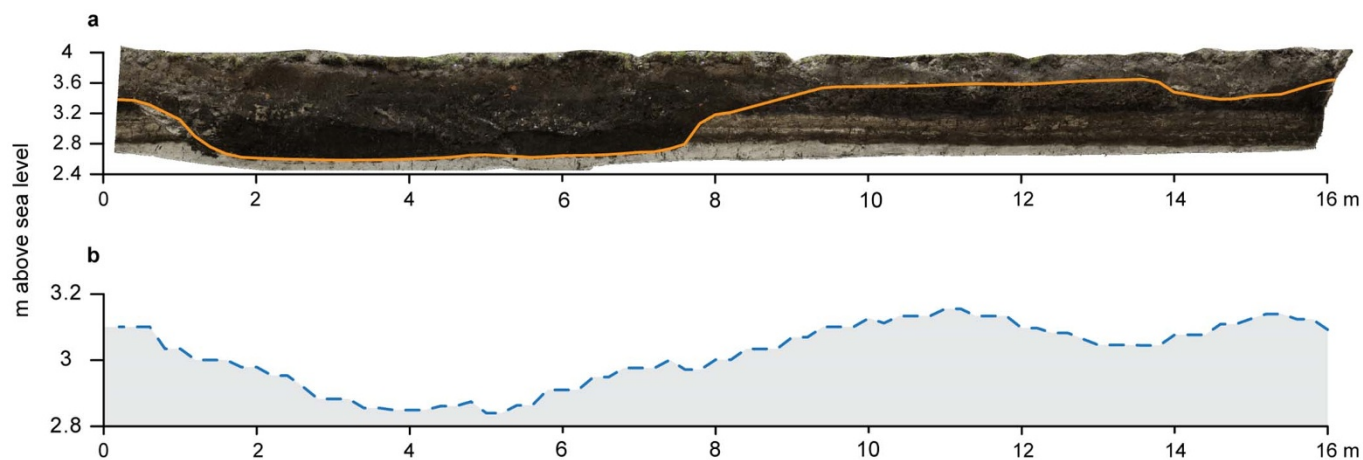


Figure 3 | Medieval terrain model evaluation. (a), Geometrically correct visualisation of the western profile of the northern moat ditch in S2 (Supplementary Fig. 2b). 84 calibration points, 0.2 m apart, along the targeted archaeological surface (orange line), were used to validate the surface model. (b), modelled medieval surface. Note the difference in y-scale between (a) and (b), which indicates the smaller standard deviation of the modelled depths (standard deviation = 0.10 m) compared to the observed surface levels (standard deviation = 0.43 m).

Discussion

Supported only by very limited invasive research, this reconstruction gives a comprehensive and unique insight into a designed medieval environment and shows, despite its transient nature, the amount of effort that was put into it. Our results also underline the discrepancies that can exist between historical information and uncovered archaeological realities that can contribute to understanding the response of past societies to social and environmental changes. The 3-D mapping of multiple soil properties, combined with limited and directed invasive research, provides a broad foundation for further geoarchaeological research. In the future, this methodology could be optimized by integrating additional physical soil properties, such as dielectric permittivity, with the σ_a and κ_a data. With the incorporation of the presented approach into different studies and environments, our knowledge of past human-landscape interactions can be significantly improved.

Methods

EMI survey. We used a motorized setup of a Dualem-21S EMI sensor¹² to survey the study area (Fig. 1). This EMI sensor simultaneously measures σ_a and κ_a with four coil configurations, i.e. with receiver coils at 1 m, 1.1 m, 2 and 2.1 m from the transmitting coil, in two orientations, i.e. horizontal coplanar (HCP) and

perpendicular (PRP) orientation, resulting in 1 m HCP, 2 m HCP, 1.1 m PRP and 2.1 m PRP. The survey was conducted by driving across the study area along parallel lines, 0.75 m apart whereby measurements were taken every 0.25 m. During surveying, soil temperature was recorded at a depth of 0.3 m to correct for temperature variations²⁶ between survey days. The resulting measurements were drift corrected¹². These data were then interpolated to a 0.1 m by 0.1 m grid using ordinary kriging²⁷ with the software Surfer v. 10 (Golden Software). All σ_a datasets were used but only the κ_a measurements from the HCP configurations were considered, as the κ_a data of the PRP configurations had a poor signal to noise ratio.

Excavations. In August 2011 and August 2012, two excavation trenches were laid out across the most apparent σ_a and κ_a anomalies (Supplementary Figures 1,2). All profiles and unearthed brick structures were recorded using computer vision-based 3-D registration²⁸.

Depth modelling. The four σ_a measurements, representative for soil volumes down to 0.5 m, 1.0 m, 1.5 m and 3.2 m below the surface, were combined to model the depth to the soil layers below the more conductive plough layer and the peaty to clayey infilling of the ditches (Fig. 3). Based on the excavation data, the morphology of the targeted soil layers was considered representative for the medieval topography. We followed the procedure from Saey et al.²² and De Smedt et al.²⁹, based on the depth response functions of the Dualem-21S coil configurations as described by Wait³⁰ and McNeill³¹. Model calibration²³ was performed, using the observed depth to these layers obtained at 34 locations in the excavation trench at S1.

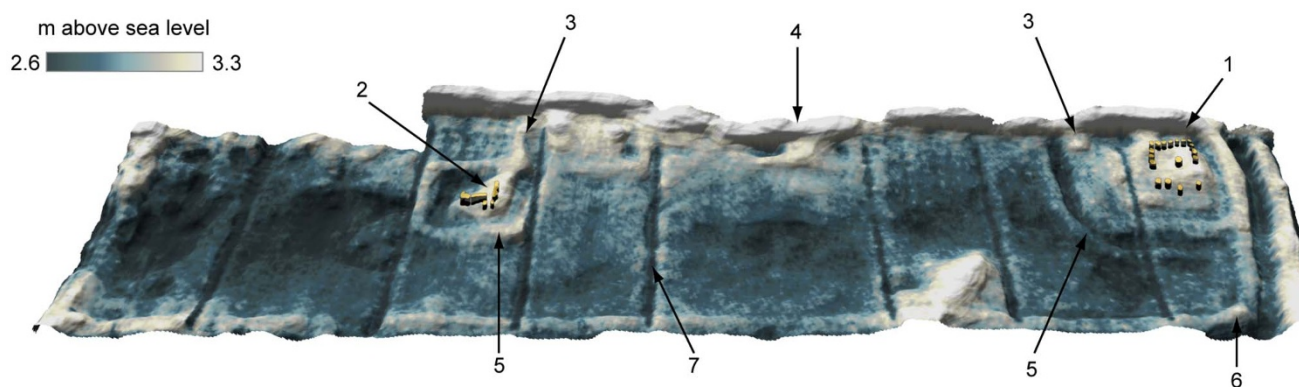


Figure 4 | Model of the medieval landscape. Three-dimensional model of the depth to the medieval surface and schematic representation of the barn and central building remains at S1 and S2, derived from the κ_a data (Fig. 2). The topographical model shows the sandy outcrop bearing structure S1 (1) and the artificially raised terrain forming the platform at S2 (2). At both sites, a pathway to the coversand ridge can be seen (3). In the north of the site the edge of the coversand ridge itself is visible (4). Moat embankments are present around both S1 and S2 (5) and a large enclosure embankment (6) surrounds the entire area. Present-day parcel ditches separate the different agricultural fields in the area (7).



1. Kvamme, K. L. Geophysical surveys as landscape archaeology. *American Antiquity* **68**, 435–457 (2003).
2. Gaffney, C. *et al.* The Stonehenge Hidden Landscapes Project. *Archaeological Prospection* **19**, 147–155 (2012).
3. Keay, S. *et al.* The role of integrated geophysical survey methods in the assessment of archaeological landscapes: the case of Portus. *Archaeological Prospection* **16**, 154–166 (2009).
4. Trinks, I. *et al.* Efficient, large-scale archaeological prospection using a true three-dimensional ground-penetrating Radar Array system. *Archaeological Prospection* **17**, 175–186 (2010).
5. Pervenier, W. La démographie des villes du comté de Flandre aux XIV^e et XV^e siècles. *Revue du Nord* **65**, 255–275 (1983).
6. Verhulst, A. *The rise of cities in North-Western Europe*. (Cambridge University Press, 1999).
7. Brenner, R. in *From peasants to farmers? The transformation of the rural economy and society in the Low Countries (middle ages-beginning 20th century) in the light of the Brenner Debate* (eds P. Hoppenbrouwers & J. L. Van Zanden) 275–338 (Brepols, 2001).
8. De Clercq, W. *et al.* Towards an Integrated Methodology for Assessing Rural Settlement Landscapes in the Belgian Lowlands. *Archaeological Prospection* **19**, 141–145 (2012).
9. *Abdij van Boudelo*. Vol. record 8 sheet 80 r°–v° (Ghent State Archives).
10. *Abdij van Boudelo*. Vol. record 6, sub no. 50 (Ghent State Archives).
11. De Belie, A. *De Boudelo abdij archeologisch onderzocht, Belsele*. (De Belie, Alfons, 1997).
12. Simpson, D. *et al.* Evaluating the multiple coil configurations of the EM38DD and DUALEM-21S sensors to detect archaeological anomalies. *Archaeological Prospection* **16**, 91–102 (2009).
13. Rhoades, J. D., Raats, P. A. C. & Prather, R. J. Effects of Liquid-phase Electrical Conductivity, Water Content, and Surface Conductivity on Bulk Soil Electrical Conductivity. *Soil Sci. Soc. Am. J.* **40**, 651–655 (1976).
14. Sudduth, K. A. *et al.* Relating apparent electrical conductivity to soil properties across the north-central USA. *Computers and Electronics in Agriculture* **46**, 263–283 (2005).
15. Fassbinder, J. W. E., Stanjekt, H. & Vali, H. Occurrence of magnetic bacteria in soil. *Nature* **343**, 161–163 (1990).
16. Le Borgne, E. Susceptibilité magnétique anormale du sol superficial. *Annales de Géophysique* **11**, 399–419 (1955).
17. Gaffney, C. & Gater, J. *Revealing the buried past. Geophysics for archaeologists*. (Tempus, 2003).
18. Le Borgne, E. Influence du feu sur les propriétés magnétiques du sol et sur celles du schiste et du granite. *Annales de Géophysique* **16**, 159–195 (1960).
19. Aspinall, A., Gaffney, C. & Schmidt, A. *Magnetometry for archaeologists*. (Altamira Press, 2008).
20. Jol, H. M. *Ground penetrating radar: theory and applications*. (Elsevier, 2009).
21. Buisman, J. *Duizend jaar weer, wind en water in de Lage Landen*. Vol. 1: tot 1300 (Van Wijnen, 1995).
22. Saey, T. *et al.* Reconstructing the paleotopography beneath the loess cover with the aid of an electromagnetic induction sensor. *Catena* **74**, 58–64 (2008).
23. De Smedt, P. *et al.* A multidisciplinary approach to reconstructing Late Glacial and Early Holocene landscapes. *Journal of Archaeological Science* **40**, 1260–1267 (2013).
24. Cassidy-Welch, M. *Monastic Spaces and their Meanings: Thirteenth-Century English Cistercian Monasteries*. (Brepols, 2001).
25. Verhaeghe, F. in *Medieval Moated Sites in North-West Europe. BAR International Series* (eds F. A. Aberg & A. E. Brown) 127–172 (Archaeopress, 1981).
26. Sheets, K. R. & Hendrickx, J. M. H. Noninvasive Soil Water Content Measurement Using Electromagnetic Induction. *Water Resour. Res.* **31**, 2401–2409 (1995).
27. Goovaerts, P. *Geostatistics for Natural Resources Evaluation*. (Oxford University Press, 1997).
28. De Reu, J. *et al.* Towards a three-dimensional cost-effective registration of the archaeological heritage. *Journal of Archaeological Science* **40**, 1108–1121 (2013).
29. De Smedt, P. *et al.* Reconstructing palaeochannel morphology with a mobile multicoil electromagnetic induction sensor. *Geomorphology* **130**, 136–141 (2011).
30. Wait, J. R. A note on the electromagnetic response of a stratified earth. *Geophysics* **27**, 382–385 (1962).
31. McNeill, J. D. *Electromagnetic terrain conductivity measurement at low induction numbers. Technical Note 6. 13* (Geonics Limited, Ontario, 1980).
32. AGIV. *DHM-Vlaanderen (2001-2004): Digitaal Hoogtemodel Vlaanderen (CD-ROM)*. (Ondersteunend centrum GIS-Vlaanderen, 2004).
33. AGIV. *Orthofoto's, middenschalig, kleur (2002), provincie Oost-Vlaanderen (CD-ROM)*. (Ondersteunend centrum GIS-Vlaanderen, 2003).

Acknowledgements

We thank Russell Palmer for his help with the text. We would also like to thank H. De Coene for granting unlimited access to his land, and thank the volunteers who assisted in the excavation campaigns. Lastly, we thank Valentijn Van Parys for assisting in the geophysical surveys.

Author contributions

P.D.S. coordinated the geophysical fieldwork and performed the geophysical data processing. P.D.S., E.M. and T.S. composed and validated the depth model. D.H. conducted the historical research. J.D.R. recorded 3-D excavation data and supplied the depth model calibration data. W.D.C. led the excavation campaign. M.V.M., P.C. and W.D.C. coordinated the research project. P.D.S., M.V.M., D.H. and W.D.C. wrote the paper. All authors commented on the results and the manuscript.

Additional information

Supplementary information accompanies this paper at <http://www.nature.com/scientificreports>

Competing financial interests: The authors declare no competing financial interests.

License: This work is licensed under a Creative Commons Attribution-NonCommercial-NoDerivs 3.0 Unported License. To view a copy of this license, visit <http://creativecommons.org/licenses/by-nc-nd/3.0/>

How to cite this article: De Smedt, P. *et al.* The 3-D reconstruction of medieval wetland reclamation through electromagnetic induction survey. *Sci. Rep.* **3**, 1517; DOI:10.1038/srep01517 (2013).